VISIBLE AND NEAR-IR SPECTRAL REFLECTANCE OF GEOLOGICALLY IMPORTANT MATERIALS

A SHORT REVIEW.

Robert B. Singer

Planetary Geosciences
Hawaii Institute of Geophysics
2525 Correa Rd.
Honolulu, HI 96822

INTRODUCTION

A number of extensive surveys of the reflectance properties of geologically interesting materials exist in the literature. The purpose of this paper is to provide a short review and to serve as a resource for readers interested in further details. Excellent review papers have been written by Adams (1975) and Hunt (1977). A library of reflectance spectra of many phases was published in a series of papers by Hunt and Salisbury (1970,1971) and Hunt et al. (1971, 1973a,b,c, 1974). While the utility of these data is somewhat limited by the lack of chemical and/or other characterizations of the samples, this series of papers provides a good starting point for more detailed studies. Spectra obtained in the field of plutonic igneous rocks have been published by Blom et al.(1980). Burns (1970) and Burns and Vaughan (1975) provide detailed discussion of some of the physical mechanisms which control spectral reflectance.

A note of caution is appropriate at this point: the researchers referenced above obtained their data using different equipment, illumination geometries, and sample preparations. A discussion of some grain size and geometry effects is provided by Adams and Felice (1967). In general the measurements of Adams are diffuse reflectance of powders, those of Hunt and his co-workers are bidirectional reflectance of powders, those of Blom et al. are bidirectional reflectance of natural rock surfaces, and those of Burns are mainly transmission of polarized light through oriented crystals. The relationships among data taken in these various ways are not totally understood, and must be considered for each applicaton.

SOURCES OF SPECTRAL FEATURES

1) Charge Transfers and Conduction Bands.

A charge-transfer feature is generated when incident radiation is of the proper energy (wavelength) to cause an electron to hop between neighboring ions. Common ion pairs include $Fe^{3+} \rightarrow O^{2-}$ and $Fe^{3+} \rightarrow Fe^{2+}$. Absorption bands of the former are centered in the near-U.V. (relatively high energy) and are quite intense, while the latter occur between 0.55 and 0.80 μm (somewhat lower energies) and are less intense (Burns et al.,1976).

For some materials, particularly semiconductors, visible or near-IR photons have enough energy to boost electrons into a conduction band, where they are no longer bound to a specific ion. Sulphur and sulphur compounds are examples. They have a steep absorption edge in the visible, with high reflectance at longer wavelengths (lower energies) and strong absorption at shorter wavelengths (higher energies).

2) Crystal Field Absorptions.

Crystal field absorptions are intraelectronic events in which anion electrons are excited into a higher energy orbital by incident radiation. Orbital energy levels

are modified by electrostatic repulsion from the surrounding anions. Different crystal structures, with varied cation site symmetries and cation-anion distances, have different "crystal fields" which control the location, strength, and width of the absorption bands. Most important crystal-field absorptions are due to elements in the first transition series, most notably ferrous iron, in somewhat distorted octahedral coordination with oxygen. Many of the Fe^{2+} crystal field bands are relatively broad and occur near 1 μm. A detailed discussion of mineralogic applications of crystal field theory is provided by Burns (1970).

3) Vibrational absorptions.

Stretching and bending vibrations of molecular bonds have discrete excitation energies, corresponding to specific wavelengths of radiation. This fundamental mode for most bonds of geologic interest (Si,Al,Mg to oxygen) occurs at wavelengths beyond the near-infrared, with overtone absorptions too weak to observe in this spectral region. While the fundamentals for OH (near 2.75 μm) and H_2O (near 3 and 6 μm) are also beyond this region, various overtones and combinations can be prominent in the near-IR. Overtones and combination vibrations of the C-O bond are also seen in the near-IR for carbonate minerals. These various absorptions will be discussed further in the context of specific minerals. An excellent discussion of vibrational spectral features can be found in Hunt (1977).

DISCUSSION BY MINERAL GROUP

Examples of reflectance spectra of various mineral groups are presented here. Unless otherwise noted, spectra are of particulate samples observed with a bidirectional instrument.

1) Pyroxenes

The prominent spectral characteristic of most pyroxenes is the occurance of two ferrous iron crystal-field absorptions, one near 1 μm and the other near 2 μm. Adams (1974) demonstrated a strong empirical relationship between center position of these two bands and pyroxene composition. Cations occur in pyroxene in 6-fold coordination with oxygen in two separate mineralogic sites: a relatively undistorted site (M1) and a more highly distorted site (M2).

Figure 1a shows the spectrum of an orthopyroxene in the hypersthene range, En_{86} (Singer, 1981). The two major bands are centered near 0.92 and 1.87 μm. The Fe^{2+} preferentially occupies the more distorted (and thermodynamically more stable) M2 sites (Burns, 1970). With increasing iron content in orthopyroxenes

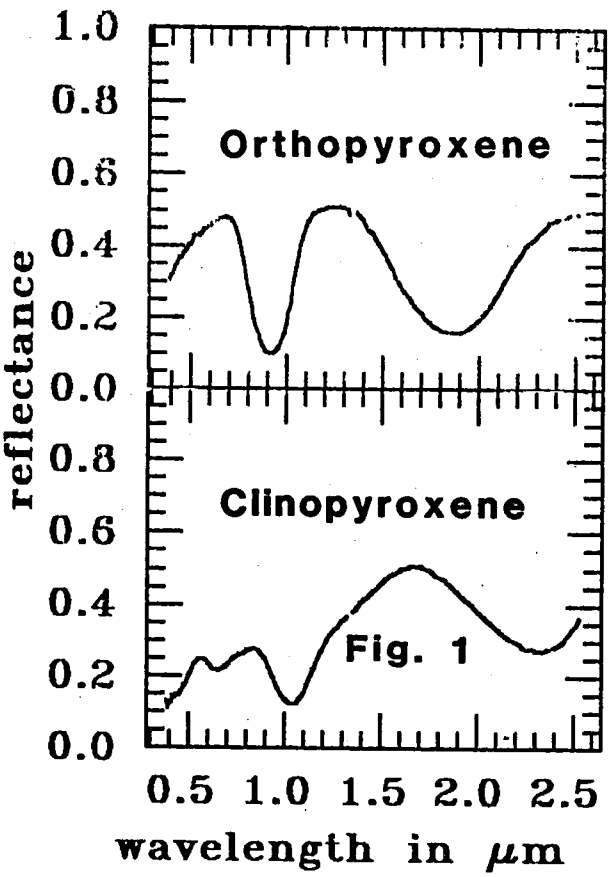

both absorptions shift to longer wavelengths. The reflectance dropoff from the red to the U.V. is most likely caused by $Fe^{2+} \rightarrow O^{2-}$ charge transfers. The narrow, weak bands superimposed on this slope are spin-forbidden Fe^{2+} crystal-field absorptions.

The spectrum of a diopsidic-augite clinopyroxene ($Wo_{41}En_{51}Fs_8$) is shown in Figure 1b (Singer, 1981). The sample contains small amounts of Al, Ti, and Fe^{3+}. The two prominent crystal-field absorptions are centered near 1.03 and 2.31 μm, consistent with the Adams (1974) relationship. Clinopyroxenes have cation sites analogous to orthopyroxenes, but Ca^{2+} preferentially fills the more distorted M2 sites, increasing the occupancy of the less distorted M1 sites by Fe^{2+}. These changes and the modified crystal structure account for the occurance of clinopyroxene absorptions at longer wavelengths than for orthopyroxene and cause a different dependence of band location on composition (Burns et al., 1972; Adams, 1975). The shallower band located near 0.65 μm is probably either an $Fe^{2+} \rightarrow Fe^{3+}$ charge transfer or a crystal-field absorption caused by a small amount of chromium.

2) Olivine

The spectrum of an olivine with composition Fo_{85} is shown in Figure 2. The three overlapping Fe^{2+} crystal-field absorptions, located at 0.86, 1.06, and 1.33μm, are diagnostic for this mineral. The weaker side bands appear as shoulders on the more intense central absorption. Assignments of these components to specific crystallographic sites and electronic transitions is provided by Burns (1970). With increasingly fayalitic composition all three absorptions shift to slightly longer wavelengths and increase in depth, with a larger proportional increase of the shoulders, leading to an overall broadening of the absorption envelope, especially on the long wavelength side (Burns, 1970; Hunt and Salisbury, 1970; Adams, 1975).

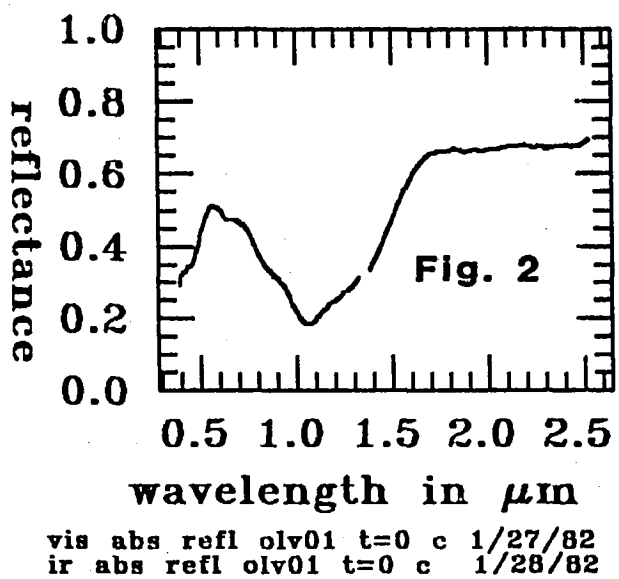

Fig. 2

3) Phylosilicates

The distinguishing characteristics of layered silicates are relatively sharp, asymmetric bands in the near-IR caused by structural OH and often molecular H_2O. As discussed above these are overtones and combinations of stretching and bending vibrational modes which have fundamentals further in the infrared. Absorptions near 1.9 μm are due to a combination of the H-O-H bend and the asymmetric O-H stretch, and are therefore indicative of adsorbed molecular water. Absorptions in the 1.4 μm region arise from O-H stretch in molecular water and/or structural OH. Band in the 2.2 - 2.4 μm region are attributed to combination overtones of structural OH stretches with lattice modes, and therefore are dependent on the cation present. For di-octahedral clay minerals (Al^{3+} bearing) a band occurs near 2.2 μm, with a weaker band frequently present near 2.3 μm. For tri-octahedral minerals (Mg^{2+} bearing) analogous absorptions appear near 2.3 and 2.4 μm.

Figure 3a is the spectrum of a montmorillonite (a di-octahedral smectite clay). Smectites generally contain a large amount of physically adsorbed molecular H_2O in interlayer sites, and therefore have a prominent absorption near 1.9 μm. The band near 1.4 μm arises from both this molecular water and the structural OH in the clay structure. The weaker band near 2.22 μm is due to the Al - OH combination mode discussed above. The reflectance falloff towards longer wavelengths is the wing of more intense water absorptions further in the infrared. The very weak structure and reflectance dropoff in the very near-IR and the visible is due to a few percent ferric iron in this sample.

The spectrum of a tri-octahedral smectite with Fe^{3+} substituting for most of the Al^{3+}, known as nontronite, is shown in Figure 3b. The 1.4 and 1.9 μm bands are the same as discussed above. The longer wavelength band is shifted slightly compared to the montmorillonite, to 2.3 μm, because of the change in cation in coordination with the structural OH. The three bands at 0.44, 0.63, and 0.95 μm are crystal-field absorptions of the ferric iron, and the steep slope in the visible is caused by $Fe^{3+} \rightarrow O^{2-}$ charge transfers.

The spectrum of kaolinite, a non-smectite di-octahedral clay, is shown in Figure 3c. Like montmorillonite this mineral has aluminum in octahedral coordination with oxygen and hydroxyl, but lacks the interlayer water sites of the smectites. Accordingly, kaolinite displays characteristic OH and Al-OH bands near 1.4 and 2.2 μm, but lacks a well developed molecular water band near 1.9 μm. The weak band at this location is caused by physical adsorption of a small amount molecular water to the fine-grained clay particles.

Figure 3d shows the spectrum of serpentine, the tri-octahedral (Mg^{2+} bearing) analog of kaolinite. Like kaolinite it displays OH absorptions at near 1.4 and beyond 2.2 μm, but has only a very weak signature of pysically adsorbed water. The spectrum in the 2.2 to 2.5 μm region is somewhat complicated, showing at least three distinct bands; I have not studied this sample in great enough detail to propose an explanation.

Minerals in the mica family generally show OH absorptions near 2.2 μm and beyond, and sometimes also the 1.4 μm OH band, although Adams (1975) suggests that sometimes iron absorptions are intense enough to mask the 1.4 μm band. The molecular water absorption at 1.9 μm is absent or very weak.

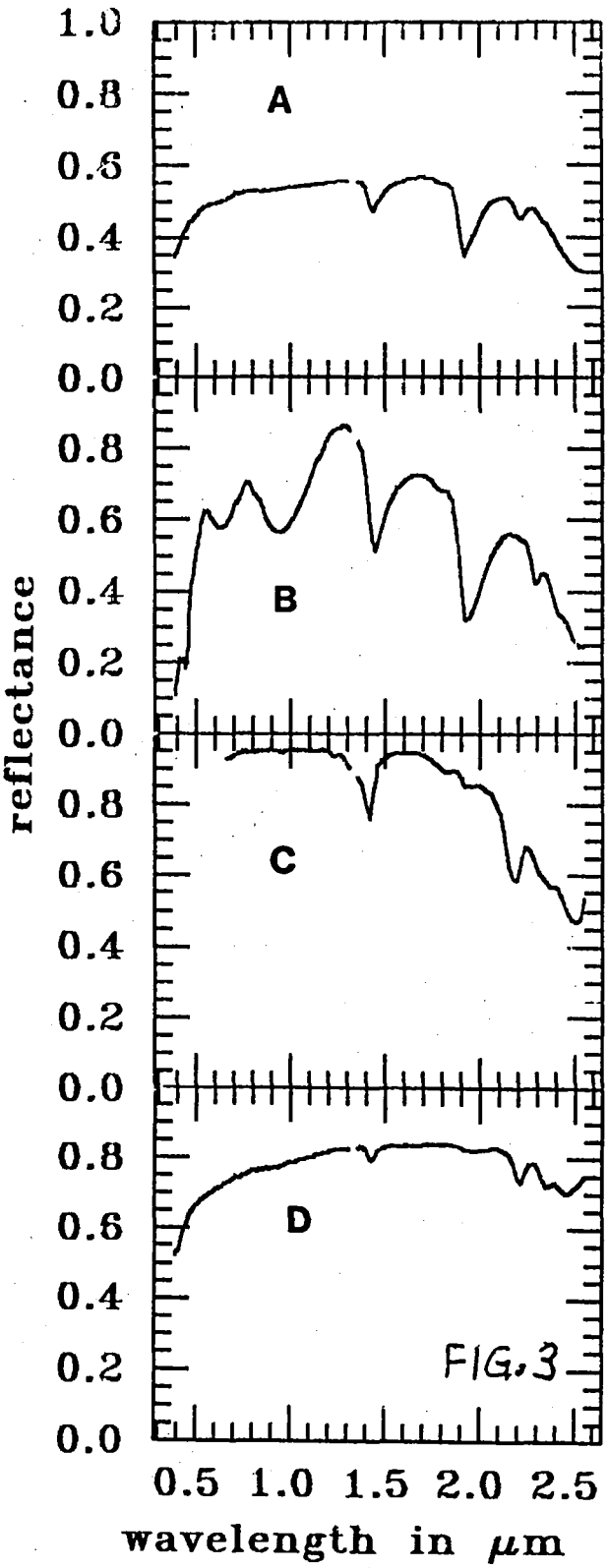

FIG. 3

4) Amphiboles

Amphiboles are hydoxylated double chain minerals somewhat analogous to the pyroxenes (single chain, non-hydroxylated). The general shape of the spectrum is often low in the visible and very near-IR due to iron absorptions, with a dramatic increase in reflectance to a spectrum peak near 1.8 to 2.0 μm. The 1.4 μm OH band is sometimes visible, apparently largely masked by the iron absorptions. A double or single absorption due to the combination of hydroxyl stretching modes and lattice modes is generally promient at 2.3 to 2.4 μm. This family of minerals has not been studied in detail by our research group. The reader is referred to Hunt and Salisbury (1970) and Adams (1975) for examples and more in-depth discussion.

5) Feldspars

While pure feldspars are spectrally very neutral, naturally occuring samples generally exhibit spectral features due to trace amounts of Fe^{2+} or Fe^{3+}, as well as liquid water inclusions. Generally K-spar accepts Fe^{3+} substitution in aluminum sites, while plagioclase more readily accomodates Fe^{2+} in calcium sites (Adams, 1975). Examples are shown in Figure 5, which was copied from Adams (1975). Trace Fe^{2+} gives plagioclase a broad absorption in the 1.1 to 1.3 μm region. There is an apparent relationship between the position of this absorption band and the albite/anorthite ratio of the plagioclase. K-spars tend to show a weak band at 0.86 μm and a relatively sharp absorption edge in the visible, both caused by trace Fe^{3+} (Adams, 1975). Because of the great transparency of most feldspars, these features are generally masked in mixtures with other minerals; the Fe^{2+} plagioclase band is often visible as a weak shoulder on the long-wavelength side of the 1 μm pyroxene band in basaltic asemblages, if there is no olivine present to hide the feldspar signature.

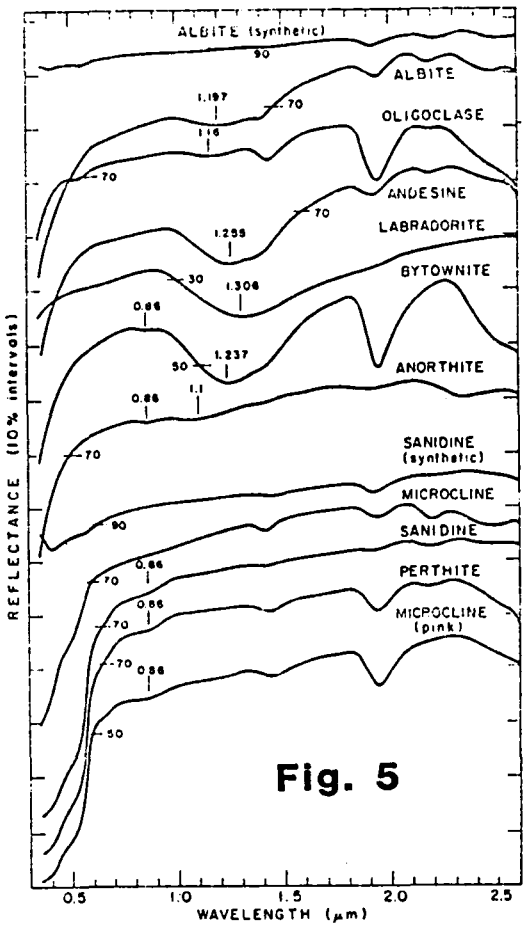

Fig. 5

6) Oxides and Hydroxides

Iron oxides and hydroxides are ubiquitous on earth and are a major source of color in rocks and soils. A few of the more common types are reviewed here.

Hematite, αFe_2O_3, (Figure 6a) has Fe^{3+} ions in octahedral coordination with oxygen. Goethite, αFeOOH, (Figure 6b) also has Fe^{3+} in octahedral coordination, although with different site distortions and oxygen ligands (OH^-), resulting in a different crystal field. Common to all reflectance spectra of fine-grained ferric oxides is strong absorption in the visible region coupled with rather high reflectance in the near infrared. The greatest contributors to this visible absorption are a pair of $Fe^{3+} \rightarrow O^{2-}$ charge-transfers centered in the near UV at 0.34 and 0.40 μm (Loeffler et al., 1974).

Both hematite and goethite display band saturation at and below 0.4 μm. The long wavelength band edge of the charge-transfers extends through the visible and into the very near infrared. Superimposed on this band edge are spin-forbidden crystal-field absorptions of Fe^{3+}. Depending on the relative positions and strengths some of these absorptions appear as shoulders or inflections on other band edges. There is a sharp unresolved doublet located at 0.53 μm in hematite and 0.45 μm in goethite. The long wavelength position of this absorption in hematite coupled with the strong charge transfer lead to a distinctive flat low reflectance profile throughout most of the visible, accounting for the intense red coloration. In goethite this crystal-field absorption occurs at a shorter wavelength and with less intensity, leading to the characteristic yellow to orange color. A second crystal-field absorption occurs for crystalline ferric oxides centered near 0.62 to 0.64 μm. In pure goethite this band is well defined; for hematite it appears only as a shoulder superimposed on the edge of the combined bands discussed above. A third crystal-field band produces a reflectance minimum at wavelengths as short as 0.86 μm for hematite to 0.89 μm or longer for goethite.

Magnetite, Fe_3O_4, (Figure 6c) is very opaque but does exhibit a shallow, broad absorption near 1 μm and a general increase in reflectance with increasing wavelength. The 1 μm band has been attributed to ferrous iron, while the continuum optical absorption has been attributed to high rate very intense charge transfers between Fe^{3+} and Fe^{2+} (Adams, 1975). The effect of opaque minerals in mixtures with other minerals will be discussed later.

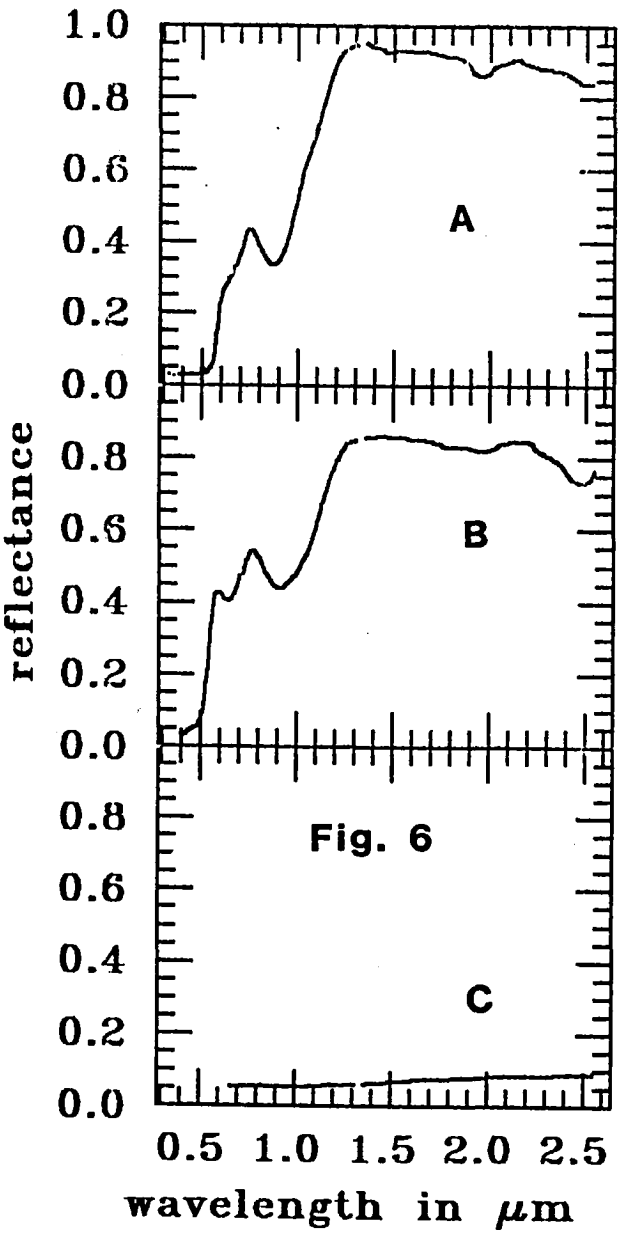

Fig. 6

7) Carbonates.

The spectral properties of carbonates are discussed in some detail by Hunt and Salisbury (1971). In this spectral region the observed absorptions occur longward of about 1.6 μm and are overtones or combinations of various modes of the CO_3^{2-} ion. As demonstrated by Figure 7a, a calcite spectrum, and Figure 7b, a dolomite, the strongest absorption occurs at a wavelength of about 2.55 μm, while the next strongest is centered near 2.35 μm. A number of additional weaker overtones occur at shorter wavelengths. An ongoing research project in our group is to investigate the systematics and uniqueness of carbonate absorption features. The calcite and dolomite examples presented here, for instance, are distinguishable by slight differences in the wavelengths of the

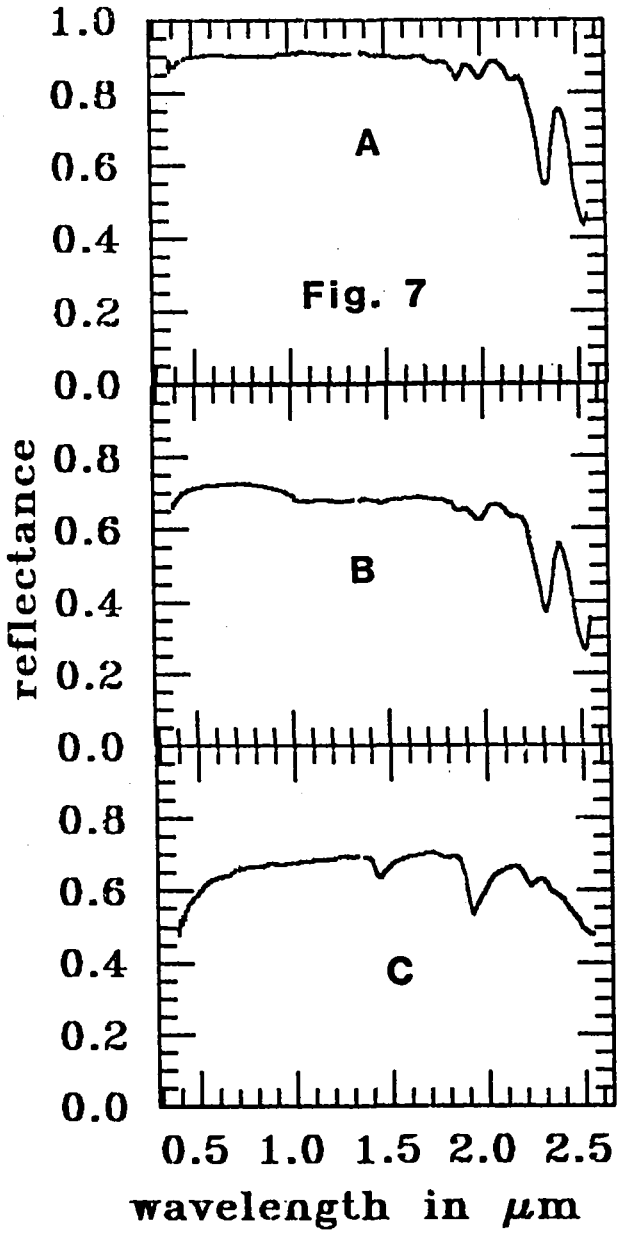

vibrational features. Both these samples show little absorpton in the visible, which indicates that they are relatively free of color producing contaminants such as iron.

Figure 7c is the spectrum of a half-and-half mixture of fine grained calcite and montmorillonite. It can be seen that in this particular mixture the clay spectral features mask most of the carbonate bands. Mixtures using coarser carbonate grains retain the features of both phases, but interpretation is still not straightforward. The deconvolution of clay and carbonate features is another area of emphasis in our current research.

MIXTURES OF MINERALS

Large scale mixing of multiple spectral components, where discrete patches of surface materials are centimeter size or larger, can be accurately treated with a simple additive or "checkerboard" model (Singer and McCord, 1979). However, intimate mixtures of several mineral components produce a net reflectance spectrum that is considerably more complicated than a simple additive or multiplicative combination of individual spectral characteristics. Investigations of lunar analog mixtures (pyroxene, plagioclase, and an opaque) have been published by Pieters (1973) and Nash and Conel (1974). Examples of laboratory mineral combinations involving two pyroxenes and a pyroxene and olivine have been presented by Adams (1974,1975). Some discussion of qualitative and quantitative analysis of spectra for mineral mixtures is also provided by Adams (1974,1975), Gaffey (1976), and Gaffey and McFadden (1977). More recently Singer (1981) presented results for laboratory mixtures of pyroxenes, olivine, and iron oxides. A few representative examples will be reviewed here.

Figure 8 shows the results of a series of weight-percent mixtures of the olivine and the clinopyroxene discussed earlier in this paper. The maximum band depth or contrast in the spectral reflectance of powders occurs when the grain size is about one optical depth (Adams and Felice, 1967). Here the overall more opaque clinopyroxene is closer to that condition than is the olivine, and therefore the spectra of mixtures are dominated by pyroxene characteristics. Because the band minima near 1 μm for these two minerals are close, there is little change in the locations of the mixture band minima. The shape and width of the total absorption envelope, however, change dramatically as

the olivine sidebands are masked by increasing pyroxene content. With pyroxene contents of 50% and greater the main indication of olivine is the depression or shoulder centered near 1.3 μm.

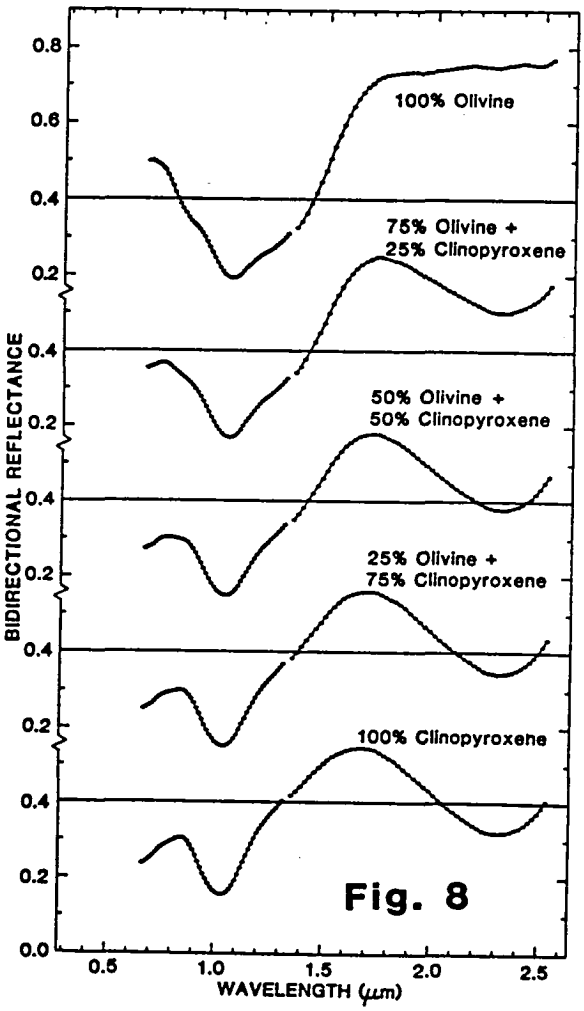

Fig. 8

An example of a mixture with an opaque phase is demonstrated in Figures 9 and 10. The albedo and spectral contrast of olivine is lowered drastically by admixture of even a small amount of magnetite. However, as shown in Figure 10, the characteristic olivine spectral shape is recognizable even in a half-and-half mixture. This behavior, which holds for pyroxenes, clays, and other phases with diagnostic spectral features, demonstrates the desirability of high precision and low noise in remotely sensed data.

Theoretical modeling of the spectral properties of mineral mixtures has advanced substantially in the last year or two. Johnson (1982) has developed a computational scheme, based on the reflectance theory published by Hapke (1981), which yields reasonable approximations to the measurements of Singer (1981). At this stage the model works somewhat better for materials of similar extinction coefficients, such as olivine and pyroxene, than it does when one component is an opaque, such as olivine and magnetite.

Another mixing geometry that is routinely encountered in the field is that of surface weathering or coatings on rocks. This problem is currently being investigated for application to Mars as well as the earth. Initial work shows that thin colored coatings, such as those bearing Fe^{3+}, exhibit wavelength dependent transmission and do not completely hide the spectral characteristics of the underlying rock (Evans et al., 1981; Singer, 1982). Laboratory work is now in progress to facilitate more quantitative modeling of this reflectance geometry.

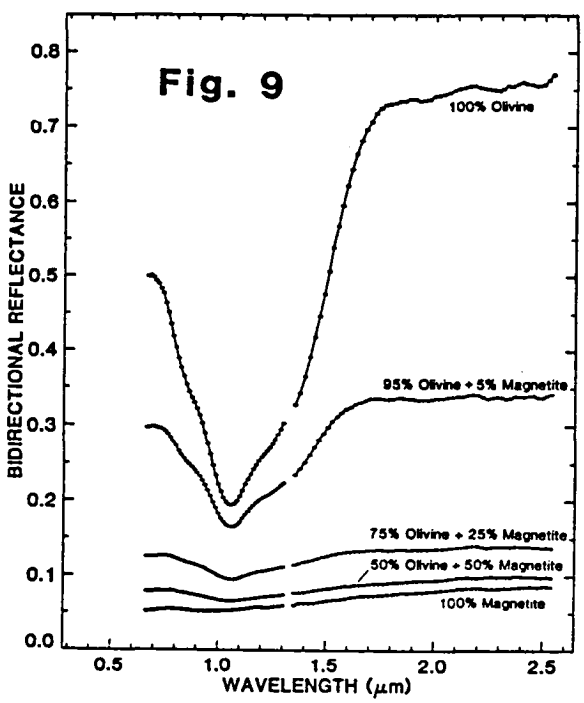

PRIORITIES FOR THE FUTURE

At present laboratory investigations of mineral and rock spectral behavior, while incomplete, outstrip our ability to make high quality remote observations in the real world. This is not to say that there isn't need for continuing laboratory research; I would, however, suggest two

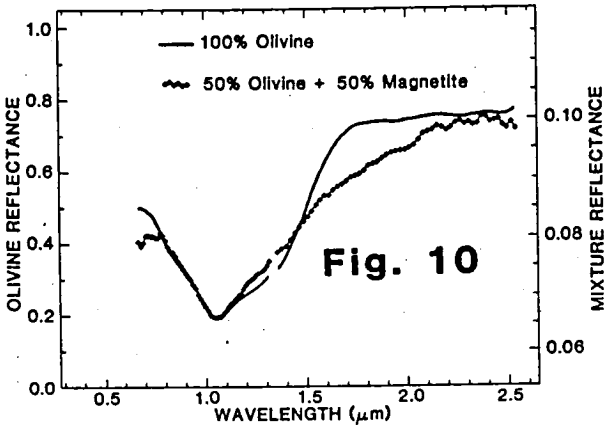

Fig. 10

complementary research directions which could over the next few years greatly enhance our abilities in geologic remote sensing:

1) Perhaps the most important laboratory research now is to refine our qualitative and especially our quantitative models of how mineral signatures combine to produce "real-world" spectral properties. This work is essential to the sophisticated capabilities for which we are all striving.

2) More on the technological side, we need to refine our remote observing techniques in terms of more complete spectral coverage, higher spectral resolution, better data precision, and more accurate calibration and atmospheric correction.

REFERENCES

Adams, J.B., Visible and near-infrared diffuse reflectance spectra of pyroxenes as applied to remote sensing of solid objects in the solar system, *J. Geophys. Res., 79,* 4329-4336, 1974.

Adams, J.B., Interpretation of visible and near-infrared diffuse reflectance spectra of pyroxenes and other rock forming minerals, in *Infrared and Raman Spectroscopy of Lunar and Terrestrial Minerals,* edited by C. Karr, Jr., Academic, New York, 91-116, 1975.

Adams, J.B., and A.L. Felice, Spectral reflectance 0.4 to 2.0 microns of silicate rock powders, *J. Geophys. Res., 72* 5705-5715, 1967.

Blom, R.G., M.J. Abrams, and H.G. Adams, Spectral reflectance and discrimination of plutonic rocks in the 0.45 to 2.45 micron region, *J. Geophys. Res., 85,* 2638-2648, 1980.

Burns, R.G., *Mineralogical Applications of Crystal-Field Theory,* Cambridge University Press, New York, 1970.

Burns, R.G., R.M. Abu-Eid, and F.E. Huggins, Crystal field spectra of lunar pyroxenes, *Proc. Lunar Sci. Conf. 3rd,* 1, 533-543, 1972.

Burns, R.G., and D.J. Vaughan, Polarized electronic spectra, in *Infrared and Raman Spectroscopy of Lunar and Terrestrial Minerals,* edited by C. Karr, Jr.,Academic, New York, 39-68, 1975.

Burns, R.G., K.M. Parkin, B.M. Loeffler, I.S. Leung, and R.M. Abu-Eid, Further characterization of spectral features attributable to titanium on the moon, *Proc. Lunar Sci. Conf. 7th,* 2561-2578, 1976.